

Optical Physical-layer Network Coding over Fiber-Wireless

Zhixin Liu⁽¹⁾, Lu Lu⁽²⁾, Lizhao You⁽²⁾, Chun-Kit Chan⁽¹⁾, and Soung-Chang Liew⁽¹⁾

⁽¹⁾ Dept of Information Engineering, The Chinese University of Hong Kong. zxliu@ie.cuhk.edu.hk

⁽²⁾ Institute of Network Coding, The Chinese University of Hong Kong. lulu@inc.cuhk.edu.hk

Abstract We propose and experimentally demonstrate the first optical physical-layer network coding (OPNC) prototype to boost throughput in an OFDM fiber-wireless network. Our technique does not require symbol-level synchronization and only requires moderate modifications of the packet preamble in IEEE 802.11 standard specification.

Introduction

Hybrid fiber-wireless (FiWi) network is a promising technology for providing ubiquitous high-capacity connectivity for mobile terminals, wireless local area networks (WLANs), and fixed wireless access services¹. The access point (AP) in a FiWi network only serves as an analog front-end that directly converts the wireless signals into optical signals without demodulation. An issue is how best to transmit these wireless-overlaid optical signals to their destinations.

Recently, physical-layer network coding (PNC) has attracted much attention in the wireless communication community. It emulates full-duplex transmission in a two-way relay channel (TWRC) by allowing two communicating users in a star-topology network to transmit signals to each other simultaneously². Doing so greatly improves the network throughput. With a similar network topology, the throughput of FiWi networks can also be improved with PNC.

Conventional PNC is realized by electronic logic operations at the relay (i.e., PNC router³), as shown in Fig. 1(a). However, in FiWi, the signals arriving at the PNC router are optical signals, and optical logic operations⁴ require stringent synchronization and complicated optical signal processing. Recently, we have successfully demonstrated an optical physical-layer network coding system⁵ named OPNC. In OPNC, the optical signals from the two communicating users are coupled together. The superimposed optical signals are then broadcasted to the two users. Each of the users then obtains the signal from the other user by subtracting its own signal from the superimposed signals.

In this paper, we incorporate the key concept of OPNC in a FiWi network. Unlike our previous demonstration, our current prototype adopts the Orthogonal Frequency Division Multiplexing (OFDM) frame format as specified in the widely adopted 802.11n WLAN standards. Binary phase-shift keying (BPSK) and quadrature phase-shift keying (QPSK) are assumed in our system.

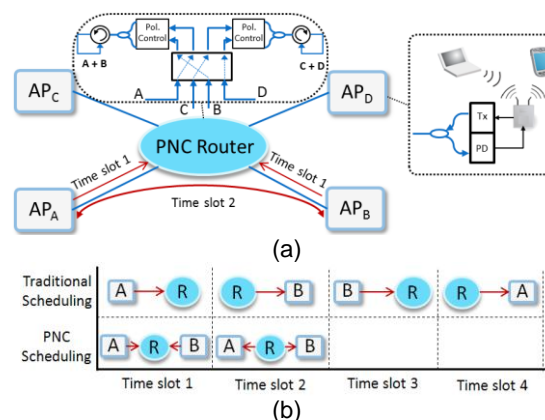


Fig. 1: (a) Proposed system architecture. (b) Comparison of the scheduling approach

To the best of our knowledge, this is the first feasibility demonstration of OFDM OPNC in FiWi networks. Notably, our OFDM OPNC scheme does not require symbol-level synchronization of the OFDM packets, and only requires moderate modifications of the packet preamble in 802.11 OFDM physical layer specifications (PHY).

Principle of Operation

Consider a four-node network as depicted in Fig. 1(a). Four APs are connected through a single router in a star topology. Suppose that node A (AP_A) and node B (AP_B) want to exchange two packets with each other. Fig. 1(b) compares traditional scheduling and PNC scheduling for this purpose. In traditional scheduling, node A sends its packet P_A to the PNC router in the first time slot. The PNC router then forwards it to node B in the second timeslot. Two more time slots are needed for the delivery of packet P_B from node B to node A in a similar fashion. A total of four timeslots are needed. PNC scheduling can achieve the same goal with two timeslots. In the first time slot, nodes A and B transmit their packets simultaneously to the PNC router. Let x_A and x_B denote the signals of packets P_A and P_B , respectively. These signals are superimposed on each other to form $y_R = x_A + x_B$, the arithmetic sum of the two signals. The router then broadcasts y_R to both

nodes A and B in the second timeslot. After receiving y_R , node A then extracts x_B by subtracting its locally pre-stored information x_A from y_R . Node B obtains x_A in a similar fashion. Note that no additional physical-layer processing other than simple optical power addition is performed at the optical PNC router. Hence, the complexity of the optical PNC router is kept low while the throughput is doubled.

At the PNC router, an optical switch is used to form multiple TWRCs, each with two end nodes exchanging information. To realize the addition operation in a direct-detection optical system, two polarization controllers are employed to control the signal polarization, so that the signals from nodes A and B are in orthogonal polarization before being power-combined via an optical coupler. An optical circulator is used to loop back the composite signal for broadcast back to both nodes A and B. In a star-topology networks with N nodes. N/2 TWRCs can be formed at the same time. PNC doubles the throughput of each TWRC. Thus, the total network throughput can be doubled given paired traffic patterns.

In our OFDM OPNC system, we avoid tight synchronization between the end nodes to simplify implementation. This means the signals from two end nodes can arrive at the PNC router with slight offset in arrival time. Fig. 2(a) illustrates the situation. Here, x_A and x_B are the OFDM symbols with relative arrival-time offset τ . The overlapped composite signal is

$$y_R(t) = x_A(t - \tau) * h_A(t) + x_B(t) * h_B(t) + \omega(t) \quad (1)$$

where $h_A(t)$ and $h_B(t)$ are the channel responses for nodes A and B, respectively, and $\omega(t)$ is the additive noise. As the data are embedded in the frequency domain, discrete Fourier transform (DFT) is performed at node A as well as node B to retrieve the spectral information. As long as τ is within the OFDM cyclic prefix (CP), the signal obtained is

$$Y_R(k) = X_A(k)e^{-j(2\pi k/N)\tau} H_A(k) + X_B(k)H_B(k) + \omega(k) \quad (2)$$

where k is the subcarrier index. Node A and node B can then obtain $X_B(k)$ and $X_A(k)$ respectively by self-information cancellation, provided that the channel responses and phase offset can be estimated from the packet preambles.

Fig. 2(b) depicts the proposed OFDM OPNC frame design. The OFDM OPNC system requires the relative delay spread τ to be within the CP duration. This can be achieved through a simple media access control (MAC) protocol. The payloads from nodes A and B contain 1280 OFDM samples, which correspond to 16 OFDM symbols for IDFT of 64 points with 16 as the CP

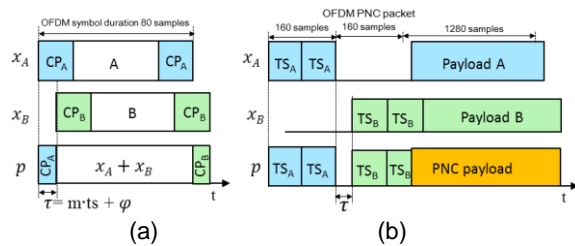


Fig. 2: (a) Illustration of OFDM symbol misalignment (b) Packet design for OFDM OPNC

length. The header of the packet from node A contains 2 training symbols for time synchronization, followed by a blank of 320 samples to avoid any temporal overlapping with the training symbols of the packet from node B. In this way, the frequency domain channel responses $H_A(k)$ and $H_B(k)$ can be estimated.

Experimental Setup

Fig. 3 shows the experimental setup. The waveforms and constellation diagrams are shown in the insets. The output of a distributed feedback laser diodes (DFB-LDs) at 1550.92 nm was split into two branches to emulate the light source of AP_A and AP_B . The continuous waves (CWs) were modulated, via two Mach-Zehnder modulators (MZMs), driven by electrical OFDM signals generated from an arbitrary waveform generator (AWG) operating at 12GS/s. The OFDM samples were generated offline using 64-point DFT. Out of the 64 subcarriers, the central 56 subcarriers were selected as data subcarriers. The signals were designed with a symbol rate of 6.25 MHz and were digitally up-converted to 2.412-GHz RF carrier frequency. The output optical OFDM signals were then amplified to 3 dBm, via their respective EDFAs, followed by a 0.8-nm optical bandpass filters (OBPF) and a polarizer in each branch to generate linearly polarized optical OFDM signals. The linearly polarized OFDM packet A and B were then launched into two reels of single mode fibers (SMF) of 8.883 km and 5.512 km, respectively. At the PNC router, two PCs controlled the polarizations of the signals from nodes A and B to ensure they were orthogonally multiplexed at the optical coupler. The upper arm of the coupler was connected to a polarization beam splitter (PBS) for polarization monitoring, while the lower arm was connected to an optical circulator fiber loop to generate the OPNC composite signal, via simple power addition. Another optical circulator was inserted in branch B to direct the OPNC composite signal into another reel of 8.832-km SMF, before was directly detected by a photon diode (PD). The detected signal was then sent over a 1-m wireless link, via a pair of isotropic antennas.

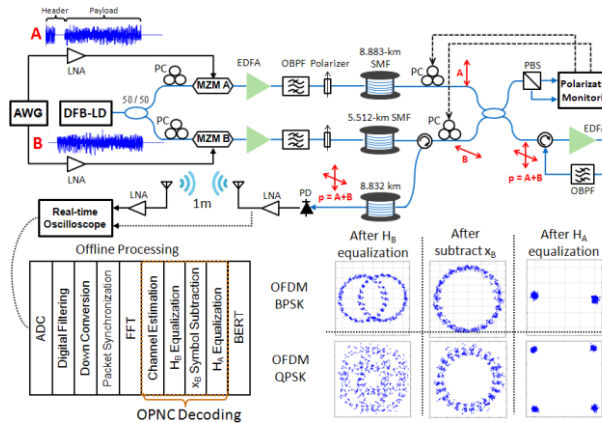


Fig. 3: Experimental setup.

The received wireless signal was then sampled at 25 GS/s by a Tektronix DSA72004 digital serial analyzer (DSA). Decoding was implemented by offline digital signal processing, and the bit-error-rate (BER) was determined based on offline error counting.

The block diagrams of digital signal processing for signal decoding is shown in the lower part of Fig. 3. The received samples were digitally down-converted to the baseband by multiplication with sine and cosine RF samples (i.e., downconversion by shifting the RF signal to baseband). Packet boundary was identified by finding the peak of the cross-correlation results between the received samples and the known training samples. The time shift between packet A and packet B was around 7 ns. The channel responses $H_A(k)$ and $H_B(k)$ were estimated using the preambles. In the experiment, we performed both OFDM-BPSK and OFDM-QPSK transmissions. For simple explanation, let's focus on the OFDM-BPSK example to elaborate the decoding process. Without loss of generality, let us focus on the decoding process at AP_B . As shown in the left-upper constellation diagram of Fig. 3, after DFT, $Y_R(k)H_B^{-1}(k)$ was computed. As can be seen $Y_R(k)H_B^{-1}(k)$ for different k yields a constellation diagram of two circles, which were attributed to the term $e^{-j(2\pi k/N)m}$ in equation (2). The radiuses of the two circles corresponded to the effective signal amplitude of $X_A(k)$. Then, with respect to the middle-upper constellation diagram of Fig. 3, a circular constellation diagram, representing $Y_A(k) = Y_R(k)H_B^{-1}(k) - X_B(k)$, was observed by subtracting the local information $X_B[k]$ from $Y_R(k)H_B^{-1}(k)$. Finally, we performed an equalization on $Y_A(k)$, i.e., by multiplying the channel inverse response $H_B(k)H_A^{-1}(k)e^{j(2\pi k/N)m}$ to $Y_A(k)$ to get a clear constellation diagram.

Experimental Results and Discussions

Fig. 4(a) shows the measured BER curves for

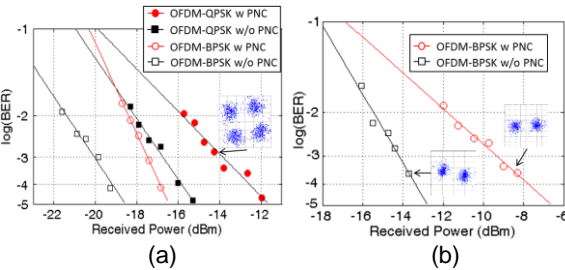


Fig. 4: BER performance of the OFDM signals with and without OPNC: (a) Without wireless transmission, (b) With wireless transmission

packet A and B, with and without our proposed OPNC scheme, with and without wireless transmission and reception. Fig. 4(b) shows the results with wireless transmission. The BER was averaged over 102 packets, which corresponding to a total of 91392 and 182784 bits for BPSK and QPSK, respectively. For the case without going through the wireless channel, receiver sensitivities at BER of 10^{-3} for OFDM-BPSK and OFDM-QPSK without OPNC were -20.03 dBm and -16.84 dBm, respectively. The receiver sensitivity for transmission with OPNC were -17.50 dBm and -13.82 dBm, respectively. The power penalties for OPNC compared to point-to-point communication are introduced by the OPNC-ASE beating noise as described in equation (4) in the previously study⁵. For the signal undergone wireless channel, the BER sensitivities for OFDM-BPSK with and without OPNC were -9.42 dBm and -14.26 dBm, respectively. The power penalties after wireless transmission were attributed to both OPNC-ASE beating noise and the wireless penalties such as fading and wireless interference.

Summary

We have demonstrated the first OFDM OPNC implementation in a star-topology FiWi system. The OFDM OPNC scheme can double the system throughput. Tight symbol-level synchronization is not needed thanks to the use of OFDM.

Acknowledgement

The project was supported by AoE Grant E-02/08, and GRF 414911 from Hong Kong RGC.

References

- [1] C. Lim et al., J. Lightwave Technol. **28**, 390-405 (2010).
- [2] S. Zhang, et al., Proc. MOBICOM, (2006).
- [3] L. Lu, et al., Physical Communication., **6**, 74-87 (2013).
- [4] Y. An, et al., Proc. OFC'13, JW2A (2013).
- [5] Z. Liu, et al., Photo. Technol. Lett., **24**, 1424-1427 (2012)

